

1 **Single-chain fluorescent integrators for mapping G-protein-coupled receptor agonists**

2

3 **Authors:** Kayla Kroning^{1,2*}, Noam Gannot^{1,3*}, Xingyu Li^{1,3,4}, Guanwei Zhou^{1,5}, Jennifer Sescil^{1,2},
4 Aubrey Putansu^{1,2}, Jiaqi Shen^{1,2}, Avery Wilson¹, Hailey Fiel¹, Peng Li^{1,3,4#}, Wenjing Wang^{1,2,5#}

5

6 *These authors contributed equally

7 #Corresponding authors

8

9 ¹Life Sciences Institute, University of Michigan, Ann Arbor, MI

10 ²Department of Chemistry, University of Michigan, Ann Arbor, MI

11 ³Department of Biologic and Materials Sciences & Prosthodontics, University of Michigan, Ann
12 Arbor, MI

13 ⁴Department of Molecular and Integrative Physiology, University of Michigan, Ann Arbor, MI

14 ⁵Program in Chemical Biology, University of Michigan, Ann Arbor, MI

15

16 **Abstract**

17

18 GPCRs transduce the effects of many neuromodulators including dopamine, serotonin,
19 epinephrine, acetylcholine, and opioids. The localization of synthetic or endogenous GPCR
20 agonists impacts their action on specific neuronal pathways. In this paper, we show a series of
21 single-protein chain integrator sensors to determine GPCR agonist localization in the whole brain.
22 We previously engineered integrator sensors for the mu and kappa opioid receptor agonists called
23 M- and K-SPOTIT, respectively. Here, we show a new integrator sensor design platform called
24 SPOTall that we used to engineer sensors for the beta-2-adrenergic receptor (B2AR), the
25 dopamine receptor D1, and the cholinergic receptor muscarinic 2 agonists. For multiplexed
26 imaging of SPOTIT and SPOTall, we engineered a red version of the SPOTIT sensors. Finally,

27 we used M-SPOTIT and B2AR-SPOTall to detect morphine, isoproterenol, and epinephrine in the
28 mouse brain. The SPOTIT and SPOTall sensor design platform can be used to design a variety
29 of GPCR integrator sensors for unbiased agonist detection of many synthetic and endogenous
30 neuromodulators across the whole brain.

31

32 **Introduction**

33 G-protein-coupled receptors (GPCRs) are involved in a variety of physiological processes¹
34 and are crucial for neuromodulation. GPCRs transduce the effects of many neuromodulators
35 including dopamine, serotonin, epinephrine, acetylcholine, and opioids. Consequently, GPCR
36 mis-regulation is often associated with diseases²⁻⁴ with over 30% of Federal Drug Administration
37 (FDA)-approved drugs targeting GPCRs⁵. Information on synthetic and endogenous GPCR
38 agonist localization across the whole brain at high spatial resolution is essential for understanding
39 the physiological effects of GPCR synthetic drugs and endogenous GPCR signaling regulation.
40 Brain-wide detection of GPCR agonists is especially important due to the long-range volume
41 transmission of neuromodulators⁶.

42 To determine the localization of neuromodulators across the whole brain, it is ideal to have
43 a GPCR agonist integrator that can convert the transient agonist signal into a permanent mark on
44 the neurons exposed to the agonists. Permanent labeling of agonist localization has two key
45 advantages over transient labeling: 1. it allows imaging of the agonist localization across the
46 whole brain; 2. the marked neurons can be further analyzed to provide information on the gene
47 expression profile of the neuron. Such genetic information allows the discovery of new druggable
48 targets for treating GPCR mis-regulation.

49 Various methods have been developed that can provide a real time (or transient) readout
50 in the neurons exposed to GPCR agonists⁷⁻¹⁵. However, fewer tools have been developed that
51 permanently label neurons exposed to GPCR agonists, and the tools that do exist have key
52 limitations. Split fluorescent protein-based¹⁶ or transcription-based¹⁷⁻¹⁹ integrators are multi-

53 component systems, where the signal-to-noise ratio (S/N) are highly dependent on the expression
54 level of each protein component. Controlling the relative expression level of the components could
55 be experimentally challenging, requiring extensive optimization²⁰. Single protein chain-based
56 integrator systems will address the limitations of multi-component systems.

57 We previously engineered single protein chain-based integrators called M-SPOTIT
58 (**S**ingle-chain **P**rotein-based **O**pioid **T**ransmission **I**ndicator **T**ool for the **M**u opioid receptor) and
59 its brighter version, M-SPOTIT2 for detecting opioids in cell cultures^{21,22}. In this paper, we show
60 the versatility of the SPOTIT design and describe new single-protein chain fluorescent integrators,
61 including a red-fluorescent SPOTIT, an opioid-activated real-time calcium sensor, and SPOTall,
62 short for **SPOTIT** for **all** GPCRs. We also demonstrate the application of M-SPOTIT for morphine
63 detection and beta-2 adrenergic receptor (B2AR)-SPOTall for isoproterenol and epinephrine
64 detection in animal models. SPOTall provides a new integrator sensor design platform that can
65 be used for the easy engineering of a variety of GPCR agonist integrators. The SPOTIT and
66 SPOTall integrators can be used for whole brain mapping of GPCR agonists.

67

68 **Results**

69

70 **Engineering of SPOTall**

71

72 The original SPOTIT was designed to specifically detect the agonists for opioid receptors
73 (ORs). To enable the ability to detect the agonists for other GPCRs, here, we established a
74 generalizable sensor design platform that can engineer integrators for many other GPCRs, called
75 SPOTall. We established the SPOTall integrator design platform based on the sensor motif we
76 discovered and utilized in SPOTIT²¹. The sensor motif consists of circularly permuted green
77 fluorescent protein (cpGFP)²³ and nanobody 39 (Nb39)²⁴, where cpGFP fluorophore maturation
78 is inhibited by Nb39 when cpGFP and Nb39 are fused together²¹ and removal of Nb39 results in

79 a >500 times fluorescence increase²¹. This sensor motif was used in the opioid integrator M-
80 SPOTIT, in which cpGFP-Nb39 is attached to the C-terminus of the mu OR (MOR). When agonist
81 binds to M-SPOTIT, Nb39 is recruited to active MOR, removing Nb39 from cpGFP, providing a
82 fluorescent readout (Figure 1a).

83 We harnessed the irreversible fluorophore maturation and large fluorescence dynamic
84 range of the cpGFP-Nb39 sensor motif to engineer SPOTall, an integrator design platform that
85 will be suitable for GPCRs beyond MOR. Since Nb39 is selective for agonist-bound MOR and
86 does not bind to other GPCRs, the SPOTall design requires the incorporation of a conformation-
87 specific binder for the active GPCR of interest. We envisioned a SPOTall design (Figure 1a) in
88 which the conformation-specific binder's recruitment to the activated GPCR would sterically
89 hinder Nb39's interaction with cpGFP and allow cpGFP fluorophore maturation.

90 For the initial testing of the SPOTall design, we chose the B2AR due to its critical function
91 in various physiological processes²⁵. Additionally, a conformation-specific nanobody, nanobody
92 80 (Nb80), already exists with a high binding affinity for activated B2AR²⁶. We first tested the
93 control design, in which cpGFP-Nb39 is attached to the C-terminus of B2AR without insertion of
94 Nb80 (Supplementary Figure 1). As expected, the B2AR agonist, isoproterenol did not cause
95 fluorescence increase, because Nb39 is selective towards active ORs. We then tested the B2AR-
96 SPOTall design we envisioned as shown in Figure 1a with Nb80 inserted between cpGFP and
97 Nb39. We also tested another geometry with Nb80 fused after cpGFP-Nb39 (Supplementary
98 Figure 1). B2AR-SPOTall with Nb80 inserted between cpGFP and Nb39 gave significant
99 fluorescence increase upon addition of isoproterenol, while fusing Nb80 after cpGFP-Nb39 did
100 not (Fig.1a-c, Supplementary Figure 1). Therefore, Nb80 inserted in between cpGFP and Nb39
101 can better disrupt Nb39's interaction with cpGFP.

102 With the optimal placement of Nb80, we next probed different linker lengths of the linker
103 connecting B2AR to cpGFP to evaluate its effect on B2AR-SPOTall activation efficiency. We
104 compared the 10 amino acids of the KOR's C-terminus, as we previously used in M-SPOTIT²¹,

105 and the truncated linkers with 8 amino acids and 6 amino acids (Supplementary Figure 1).
106 Truncating the linker showed no significant change in the activated signal, so we moved forward
107 with the 10-amino acid linker for B2AR-SPOTall.

108

109 **Characterizations of B2AR-SPOTall**

110

111 We next characterized the various parameters important for B2AR-SPOTall's
112 performance. The agonist exposure time needed to initiate the sensor activation along with the
113 incubation time needed for fluorophore maturation are both important for SPOTall performance.
114 We previously observed that M-SPOTIT can be activated with a 30-second pulse of fentanyl
115 followed by 12 hours of incubation without fentanyl²¹. Short pulses of agonist create a stable
116 agonist-bound complex that remains after the agonist is washed from the cell media and until the
117 fluorophore has matured.

118 To characterize the agonist incubation time needed to activate B2AR-SPOTall, we
119 stimulated HEK293T cells expressing B2AR-SPOTall with isoproterenol for 30 seconds, 5
120 minutes, 6 hours, or 24 hours. After the given stimulation time, the isoproterenol was removed,
121 and the cells were further incubated for 24 hours in a media without agonist to allow the
122 fluorophore to mature. The cells were then fixed and imaged. We found as short as a 30-second
123 stimulation with agonist was sufficient to initiate the B2AR-SPOTall sensor activation (Fig. 1d).
124 However, longer agonist incubation times resulted in decreased fluorescence activation (Fig. 1d),
125 which we hypothesized was from lower protein level due to hyperstimulation of B2AR. For the
126 remaining cellular characterizations of B2AR-SPOTall, we used a 5-minute agonist stimulation
127 protocol, which is easier to perform than the 30-second stimulation and still gives a relatively high
128 fluorescent increase upon agonist stimulation.

129 To evaluate the time needed for fluorophore maturation in B2AR-SPOTall, we stimulated
130 B2AR-SPOTall expressing cells for 5 minutes followed by further incubation for differing amounts

131 of time before imaging. Clear agonist-dependent activation was observed 8-hours post
132 stimulation, reaching a plateau at around 24 hours (Fig. 1e). Moving forward, we imaged cells 24
133 hours post stimulation to give the highest sensor activation and S/N. Here, we define the S/N as
134 the ratio of the agonist-stimulated fluorescence to the unstimulated condition. Even though
135 SPOTall requires >8 hours of incubation for fluorophore maturation, the agonist needs to be
136 incubated as short as 30 seconds to form a stable complex to initiate fluorophore maturation.

137 Another parameter that is important for SPOTall's performance is the fluorophore's pKa in
138 a formaldehyde-fixed condition. We observed previously that cpGFP in fixed cells has a high pKa,
139 requiring high pH buffer to deprotonate the fluorophore to observe maximum fluorescence²¹. We
140 next measured the pKa of the B2AR-SPOTall fluorophore formed in formaldehyde-fixed
141 conditions. We performed a pH titration by imaging the stimulated B2AR-SPOTall with buffers at
142 a range of pH values. We determined the B2AR-SPOTall's pKa to be 8.3 (Fig. 1f), requiring a pH
143 >10.3 to achieve >99% deprotonation of the fluorophore. Therefore, a buffer at pH 11 is used for
144 B2AR-SPOTall imaging for all experiments.

145 To evaluate B2AR-SPOTall's selectivity for B2AR agonists, we characterized B2AR-
146 SPOTall against a variety of ligands, including FDA-approved agonists, the endogenous ligand,
147 an antagonist, and ligands selective for other GPCRs. B2AR-SPOTall was significantly activated
148 by B2AR agonists but not by the antagonist or agonists for other GPCRs (Fig. 1g), validating the
149 selectivity of the B2AR-SPOTall for B2AR agonists.

150 Lastly, to evaluate B2AR-SPOTall's sensitivity for B2AR agonists, we stimulated B2AR-
151 SPOTall with ligands of varying concentrations. The FDA-approved drugs arformoterol,
152 indacaterol, and isoproterenol all showed EC50 values of approximately 1-6 μ M (Supplementary
153 Fig. 2). B2AR-SPOTall's EC50 value for epinephrine is 10 times higher (44 μ M) compared to the
154 FDA-approved drugs. This data shows that B2AR-SPOTall is more sensitive towards synthetic
155 ligands than the endogenous agonist.

156

157 **Easy extension of the SPOTall platform to other GPCRs**

158

159 To test the generalizability of the SPOTall platform, we next applied the optimal SPOTall
160 design to other GPCRs by simply replacing B2AR and Nb80 with other GPCR-conformation-
161 specific binder pairs. We first engineered a SPOTall sensor with another G_s-coupled receptor, the
162 dopamine receptor D1 (DRD1). We reasoned DRD1's structural similarity to B2AR might allow
163 Nb80 to bind to the active DRD1. Therefore, the only change we made to the B2AR-SPOTall
164 design for DRD1-SPOTall is that we replaced B2AR with DRD1 (Fig. 2a). A significant
165 fluorescence increase was observed upon addition of dopamine with a S/N of 43. This shows that
166 Nb80 can bind to activated DRD1 intramolecularly and that the SPOTall sensor design can be
167 extended to another GPCR (Fig. 2b and c).

168 We next engineered a SPOTall sensor with another GPCR, the cholinergic receptor
169 muscarinic 2 (CHRM2). CHRM2 also has an available conformation-specific nanobody, Nb9-8²⁷.
170 We designed CHRM2-SPOTall as shown in Fig. 2a. A significant fluorescence increase was
171 observed upon addition of the CHRM2 agonist iperoxo with a S/N of 29 (Fig. 2b and c). These
172 studies show that the SPOTall platform is generalizable for GPCRs with a conformation-specific
173 binder. However, both DRD1-SPOTall and CHRM2-SPOTall have overall lower fluorescence
174 intensity than B2AR-SPOTall, necessitating further improvement before animal testing.

175

176 **Engineering of red-SPOTIT**

177

178 In addition to extending the single-chain integrator to other GPCRs, we designed a single-
179 chain red fluorescent integrator. A red fluorescent integrator will complement the green
180 fluorescent SPOTIT and SPOTall for multiplexed detection of GPCR agonists. Red fluorescent

181 sensors are also advantageous in that red wavelengths overlap less with the autofluorescence of
182 animal tissue, improving the S/N.

183 In the red-SPOTIT design, we replaced cpGFP with circularly permuted mApple
184 (cpmApple), a red fluorescent protein used in the calcium sensor, O-Geco1²⁸. Surprisingly, this
185 design showed no cpmApple fluorescence with or without opioid stimulation (data not shown). To
186 investigate this, we performed a control study of expressing cpmApple alone in comparison to
187 cpmApple fused to the calcium-dependent protein pair, M13 and CaM (the same construct as O-
188 Geco1). Interestingly, the cpmApple alone from O-Geco1 does not have fluorescent signal at pH
189 11 while O-Geco1 shows red fluorescence (Supplementary Fig. 3). The lack of fluorescence in
190 cpmApple alone is not due to protein stability since immunofluorescence indicates the protein is
191 expressed for both constructs. This suggests that the cpmApple fluorophore in O-Geco1 requires
192 fusion to M13 and calmodulin to mature. Therefore, to engineer red-SPOTIT, we need to
193 incorporate the whole O-Geco1 construct rather than just cpmApple itself.

194 To determine if Nb39 can inhibit cpmApple fluorophore maturation with M13 and
195 calmodulin added back, we added Nb39 to the C-terminus of O-Geco1 and saw significant
196 inhibition of fluorophore maturation (Supplementary Fig. 3). Additionally, protease cleavage to
197 remove Nb39 from O-Geco1 can significantly increase the red fluorescence (Supplementary Fig.
198 3). This suggests that O-Geco1-Nb39 works similarly to cpGFP-Nb39 and can be used for a
199 single-chain fluorescent integrator design.

200 To design a red opioid integrator, we fused O-Geco1-Nb39 to the C-terminus of the MOR
201 and kappa opioid receptor (KOR) (Fig. 3a). These two red fluorescent integrators are called M-
202 and K-red-SPOTIT. M- and K-red-SPOTIT each yielded a fluorescence increase upon opioid
203 stimulation with a S/N of 4.2 and 4.4, respectively (Fig. 3b and Supplementary Fig. 3).

204

205 **Engineering of an opioid-activated real-time calcium sensor**

206

207 Calcium influx is a common marker for neural activity. Consequently, many genetically
208 encoded calcium sensors have been engineered to determine neural activity in cell-type specific
209 neural populations²⁹. By combining the SPOTIT design and the widely used calcium sensor,
210 GCaMP6²³, we engineered a real-time calcium sensor that is only functional in opioid-dependent
211 neural circuits. We reasoned such a sensor can be used to detect neuronal activity induced
212 calcium influx specifically in the neuronal circuits involved in opioid signaling, offering more
213 specificity to the GCaMP sensor.

214 To design an opioid-activated calcium sensor, we replaced cpGFP in green M-SPOTIT
215 with M13-cpGFP-CaM from GCaMP6²² (Fig. 3c). In this design, the fluorophore maturation is still
216 dependent on opioid stimulation. Once the integrator's fluorophore is matured after opioid
217 stimulation, the integrator can then serve as a real-time calcium indicator, because it contains the
218 GCaMP6 elements (Fig. 3c). We call this new integrator SPOTcal.

219 To test SPOTcal, we stimulated SPOTcal expressing HEK293T cells with fentanyl to
220 induce fluorophore maturation first. We waited 24 hours for significant fluorophore maturation to
221 take place and then tested the matured SPOTcal's real-time calcium sensing ability. We
222 stimulated the cells with calcium and ionomycin to increase intracellular calcium concentration.
223 Ionomycin and calcium treatment caused a fluorescence increase in both the fentanyl and non-
224 fentanyl treated cells with higher fluorescence in the cells previously stimulated with fentanyl (Fig.
225 3d and Supplementary Fig. 4), illustrating the opioid-dependent calcium detection of SPOTcal.

226

227 **Animal application of M-SPOTIT2 and B2AR-SPOTall**

228

229 To evaluate the potential of these single-chain fluorescent integrators for detecting GPCR
230 agonists in animal models, we tested M-SPOTIT and B2AR-SPOTall in a mouse brain. We first
231 tested M-SPOTIT²² by injecting home-made adeno associated viruses (AAV) 1/2 mixed serotype
232 encoding M-SPOTIT2 into the preBötzing complex (preBötC) of a mouse brain. Due to the large

233 injection volume, viral expression occurred in regions beyond the preBötC as well. The preBötC
234 is the inspiratory rhythm generator and is impacted by opioid signaling³⁰.

235 6 days after viral injection of M-SPOTIT2, we administered morphine or saline via IP
236 injection to the mice. Then, 24 hours after morphine or saline administration, we sacrificed the
237 mice for imaging (Fig. 4a). We observed a 4.9 times signal increase in the morphine administered
238 group in comparison to the saline control group (Fig. 4b and c and Supplementary Fig. 5). Lower
239 M-SPOTIT2 protein levels were observed in the saline stimulated condition (Fig. 4b). Lower
240 protein levels in the absence of drug has previously been observed for the SPOTIT sensors³¹ and
241 is due to the instability of the inactive cpGFP-Nb39 complex. The higher signal in the morphine
242 stimulated condition is, therefore, due to both fluorophore maturation and higher sensor stability.
243 This study shows that M-SPOTIT2 can detect synthetic opioids in a mouse brain.

244 It is important to note that the SPOTIT sensors can also engage in G-protein signaling. To
245 characterize M-SPOTIT2's G-protein signaling abilities, we used the GloSensor³² assay to
246 measure cAMP levels in cell cultures. Fentanyl stimulation with M-SPOTIT2 reduces the cAMP
247 levels in HEK293T cells, indicating M-SPOTIT2 can couple to G-proteins (Supplementary Figure
248 6). To prevent G-protein coupling to M-SPOTIT2, we incorporated a series of mutations in the G-
249 protein binding pocket of MOR³³. We found one mutant, R279F, that has abolished G-protein
250 coupling while still maintaining sensor activity (Supplementary Fig. 6). These mutants can be used
251 if G-protein binding to M-SPOTIT2 becomes a concern in certain experiments. To illustrate this
252 mutation strategy works for other GPCR sensors, we applied the same strategy to the KOR
253 sensor, K-SPOTIT, where we were also able to reduce G-protein coupling to K-SPOTIT
254 (Supplementary Fig. 7). We reasoned this strategy can be used for all future SPOTall sensors if
255 G-protein coupling is a major concern.

256 Lastly, we tested the application of B2AR-SPOTall in mouse brain. AAV vector encoding
257 B2AR-SPOTall was injected into the lateral hypothalamus area. Because the activated
258 fluorescence signal and background of B2AR-SPOTall are both lower than M-SPOTIT2 in

259 HEK293T cells (Supplementary Fig. 8), we extended the viral expression time to a total of 7 days
260 before drug or saline administration (Fig. 5a). Both isoproterenol and epinephrine administration
261 induced an increase of green fluorescent signal (6.0- and 3.7-fold, respectively), compared to the
262 saline administered mice (Fig. 5b and c and Supplementary Fig. 9). Therefore, B2AR-SPOTall
263 can be applied in vivo to detect the localization of neuromodulators.

264

265 **Discussion**

266

267 Integrators for GPCR agonists are needed for whole-brain mapping of GPCR agonist
268 localization at cellular resolution and allow the analysis of neurons post signaling event, where
269 the genetic profile of the neuron can be determined. SPOTIT and SPOTall do not have time
270 gating; however, time gating can be achieved by adding temporal controls to integrators, such as
271 expressing integrators under a drug inducible promoter³⁴.

272 In this paper, we showed the design of multiple single-chain fluorescent integrators for
273 detecting GPCR agonists. In addition to our previously designed green fluorescent M-SPOTIT for
274 detecting MOR agonists, we designed SPOTall that is more generalizable for a range of GPCRs
275 and a red-SPOTIT for potential multiplexed detection. We demonstrated SPOTall's easy adaption
276 with three different GPCRs: B2AR, DRD1, and CHRM2. Notably, B2AR-SPOTall can detect as
277 short as 30 seconds of agonist stimulation and has high selectivity towards B2AR agonists. We
278 also designed an opioid-activated calcium sensor, where calcium sensing occurs only in neurons
279 previously exposed to opioids. This sensor offers important specificity to the widely used calcium
280 sensor, GCaMP6²³. To demonstrate these sensors' potential applications in mouse models, we
281 also showed the proof-of-principle applications of M-SPOTIT2 and B2AR-SPOTall in mouse
282 brains.

283 B2AR-SPOTall and M-SPOTIT2 are the first single-chain fluorescent integrators for
284 detecting GPCR agonists. They will be useful for detecting where B2AR- and MOR-targeted drugs

285 are localizing in the brain globally at cellular resolution. After further improving the sensitivity for
286 their endogenous agonists, B2AR-SPOTall and M-SPOTIT2 will also be useful for detecting the
287 release of endogenous B2AR and MOR agonists to better understand the spatial regulation of
288 endogenous signaling.

289 The SPOTall design is highly modular and can be extended to design integrators for other
290 GPCRs. While nanobodies are used as protein binders for active GPCRs in the current SPOTall
291 design, non-nanobody protein binders can also be tested in the future. Additionally, M-red-
292 SPOTIT can potentially be used at the same time as a SPOTall sensor to observe how opioid
293 signaling impacts other neuromodulator signaling events. For example, evidence has shown that
294 endogenous opioid peptides can modulate epinephrine release³⁵ and synthetic opioid agonists
295 can impact dopamine release³⁶. Red or green SPOTIT and SPOTall can also be used in
296 combination with real-time sensors to first determine the localization of GPCR agonists throughout
297 the whole brain and then perform real-time sensing of neuromodulators at those neurons. For
298 example, green SPOTIT and the red real-time dopamine sensor, RdLight1¹⁴ can be used together
299 to detect real-time dopamine release in opioid-dependent neuronal circuits. Lastly, SPOTcal can
300 label the neuronal populations relevant in opioid signaling and allow calcium imaging within those
301 neuronal populations to further study opioid-dependent neural activity.

302 Overall, SPOTall and SPOTIT provide a new single-chain fluorescent integrator platform
303 for engineering a variety of GPCR integrators. They allow mapping of GPCR agonists globally,
304 which is important for an unbiased search of endogenous agonist release and for studying drug
305 localization.

306

307 **Acknowledgments**

308

309 Kayla Kroning is supported by F31MH12915001. Noam Gannot is supported by F31HL165733-
310 01A1. Research is supported by R01DA05320001A1, HL156989 and AT011652.

311

312 **Author contributions**

313

314 Kayla Kroning and Wenjing Wang conceived the sensor designs and experimental designs for
315 HEK293T cell testing. Peng Li conceived the experimental designs for animal testing. Kayla
316 Kroning performed experiments for Fig. 1, Fig. 2, Fig. 3a and 3b, Supplementary Fig. 1, and
317 Supplementary Fig. 8. Noam Gannot determined the animal testing protocol and performed the
318 experiments for Fig. 4 and Supplementary Fig. 5. Xingyu Li performed the experiment for Fig. 5
319 and Supplementary Fig. 9. Aubrey Putansu performed the experiment for Supplementary Fig. 2.
320 Jennifer Sescil performed the experiment for Supplementary Fig. 6 and Supplementary Fig. 7.
321 Jiaqi Shen performed the experiment for Supplementary Fig. 3. Guanwei Zhou performed the
322 experiments for Fig. 3c and 3d and Supplementary Fig. 4. Hailey Fiel and Avery Wilson
323 contributed to cloning of the constructs used in these experiments. All authors participated in
324 manuscript writing and editing.

325

326 **Data Availability**

327

328 All the data supporting the findings in this manuscript are supplied within the main manuscript and
329 the supplementary information files. All the DNA constructs used in this study are available upon
330 request to the corresponding author.

331

332 **Competing Interests**

333

334 A patent has been filed by W.W. and K.E.K titled “Fluorescent biosensors and methods of use for
335 detecting cell signaling events.” U.S. Provisional Patent Application number: PCT/US22/17804.

336 Filed 02-25-2022. Applicants: The Regents of the University of Michigan. Patent pending. All

337 other authors declare no competing interests.

8

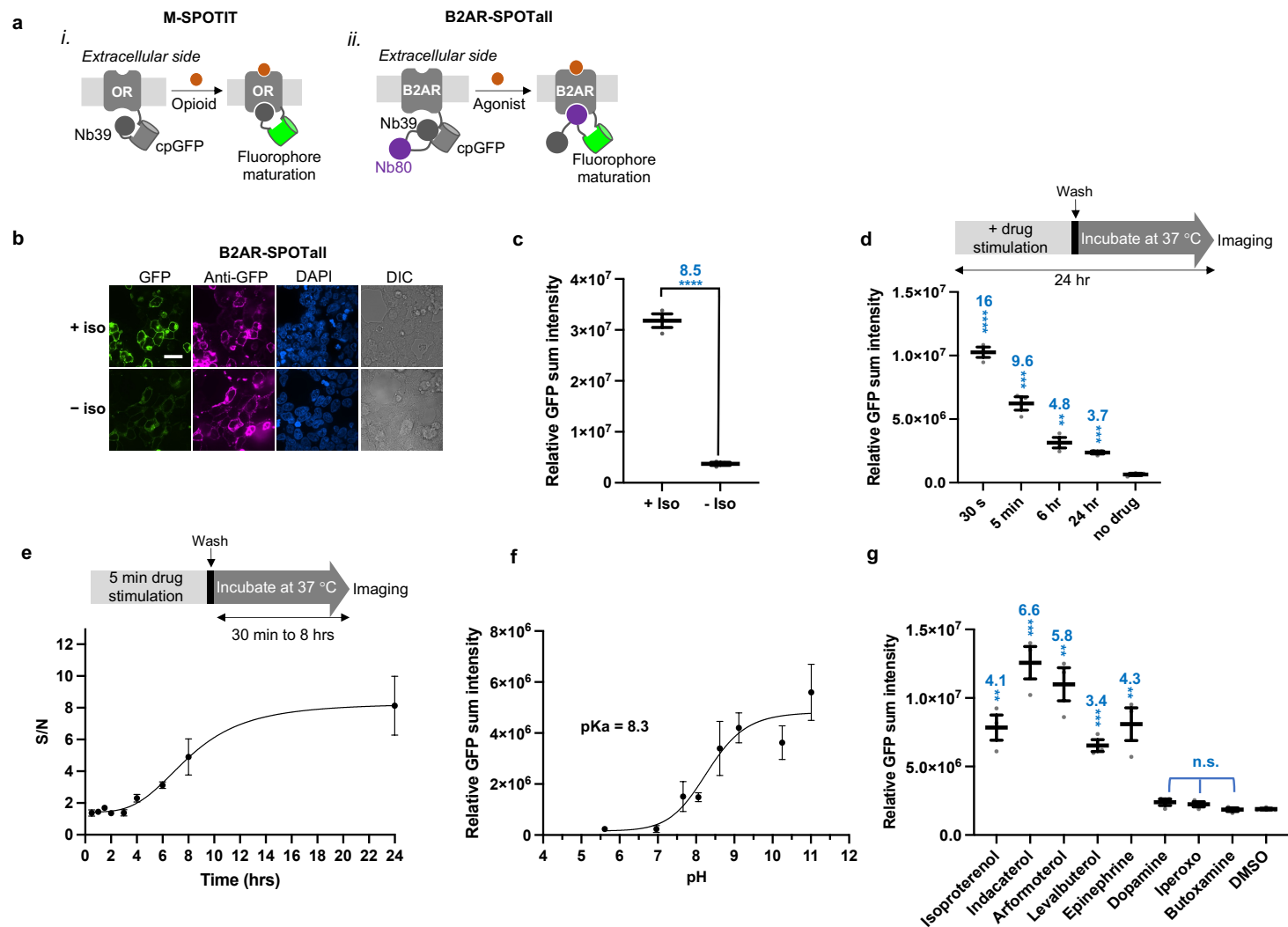


Fig. 1: B2AR-SPOTall design and characterizations. **a**, Schematic of M-SPOTIT (*i*) and B2AR-SPOTall (*ii*). For both sensor designs Nb39 inhibits cpGFP fluorophore maturation. For M-SPOTIT, opioid binding recruits Nb39 to the OR, releasing cpGFP and allowing the fluorophore to mature. For B2AR-SPOTall, agonist binding recruits Nb80, sterically blocking Nb39's interaction with cpGFP and allowing the fluorophore to mature. **b**, Testing B2AR-SPOTall in HEK293T cells. B2AR-SPOTall transfected HEK293T cells were stimulated with 10 μ M isoproterenol. 24 hours after stimulation, cells were fixed, immunostained, and imaged with pH 11 buffer. GFP, cpGFP fluorescence. Anti-GFP, protein expression level. DAPI, nuclear staining. DIC, differential interference contrast. Scale bar, 20 μ m. Iso, isoproterenol. **c**, Quantification of the experiment described in **b**. The thick horizontal bar is the mean value of three technical replicates. The number above the dots is the S/N; the stars indicate statistical significance. ****p value < 0.0001. $n = 3$. **d**, Agonist stimulation time testing of B2AR-SPOTall in HEK293T cells. Cells were stimulated with 10 μ M isoproterenol for different amounts of time, washed, and then incubated for 24 hours before imaging. Schematic of experiment is shown above the plot. The thick horizontal bar is the mean value of three technical replicates. The number above the dots is the S/N; the stars indicate statistical significance compared to the "no drug" condition. 30 s: ****p < 0.0001, 5 min: ***p = 0.0005, 6 hr: **p = 0.0042, 24 hr: ***p = 0.0003. $n = 3$. **e**, Maturation assay of B2AR-SPOTall in HEK293T cells. Cells were imaged 0.5, 1, 1.5, 2, 3, 4, 6, 8, or 24 hours post 5-minute 50 μ M isoproterenol stimulation to determine the time it would take the fluorophore to mature. Schematic of experiment is shown above the plot. $n = 3$. Dots on the plot indicate the mean value of three technical replicates. **f**, pH titration of B2AR-SPOTall expressing HEK293T cells. 24 hours post 5-minute 10 μ M isoproterenol stimulation, cells were fixed and imaged with different pH buffers: pH 5.6, 7, 7.7, 8.1, 8.6, 9.1, 10.3, and 11. Dots on the plot indicate the mean value of three technical replicates. $n = 3$. **g**, Screening B2AR-SPOTall expressing HEK293T cells against different types of ligands. Cells were imaged 24 hours post 5-minute stimulation with 50 μ M of drug. n.s., not significant. The thick horizontal bar is the mean value of three technical replicates. The number above the dots is the S/N and the stars indicate

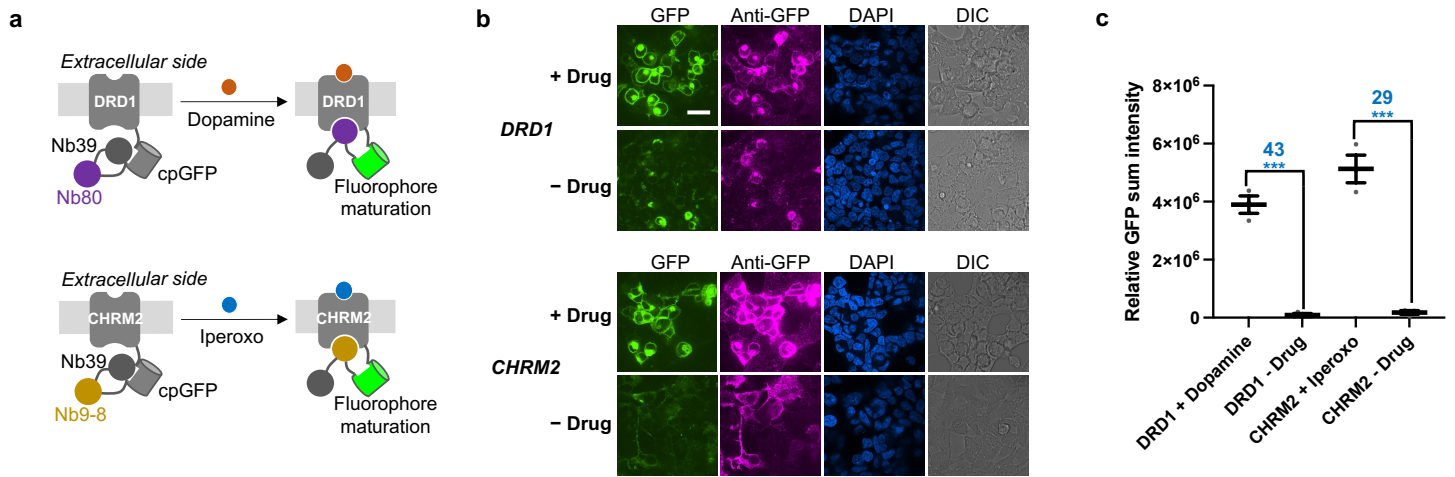
9

0

1

2

3 significance compared to the “DMSO” condition. Isoproterenol: **p= 0.0030, indacaterol: ***p= 0.0008,
4 arformoterol: **p= 0.0017, levalbuterol: ***p= 0.0004, epinephrine: **p= 0.0067, dopamine: n.s. p= 0.1196,
5 iperexo: n.s. p= 0.1580, butoxamine: n.s. p= 0.7761. $n= 3$. For c-g, error bars are the SEM and significance was
6 calculated using an unpaired, two-tailed Student’s *t*-test. A biological replicate has been performed for
7 experiments b-f that yielded similar results.



8
9 **Fig. 2: Design and testing of DRD1- and CHRM2-SPOTall.** a, Schematic of DRD1- and CHRM2-SPOTall. b, HEK293T cell testing of DRD1- and CHRM2-SPOTall. HEK293T cells expressing DRD1- and CHRM2-SPOTall
0 were stimulated with 100 μ M dopamine and iperoxo, respectively. Cells were fixed, immunostained, and imaged
1 24 hours post stimulation. GFP, cpGFP fluorescence. Anti-GFP, protein expression level. DAPI, nuclear staining.
2 DIC, differential interference contrast. Scale bar, 20 μ m. c, Quantification of b. Error bars are the SEM. The thick
3 horizontal bar is the mean value of three technical replicates. The number above the dots is S/N and the stars
4 indicate significance compared to the “- drug” condition. Significance was calculated using an unpaired, two-
5 tailed Student’s *t*-test. DRD1: ****p* value= 0.0002, CHRM2: ****p* value= 0.0005. *n*= 3. A biological replicate has
6 been performed for experiments b and c that yielded similar results.
7

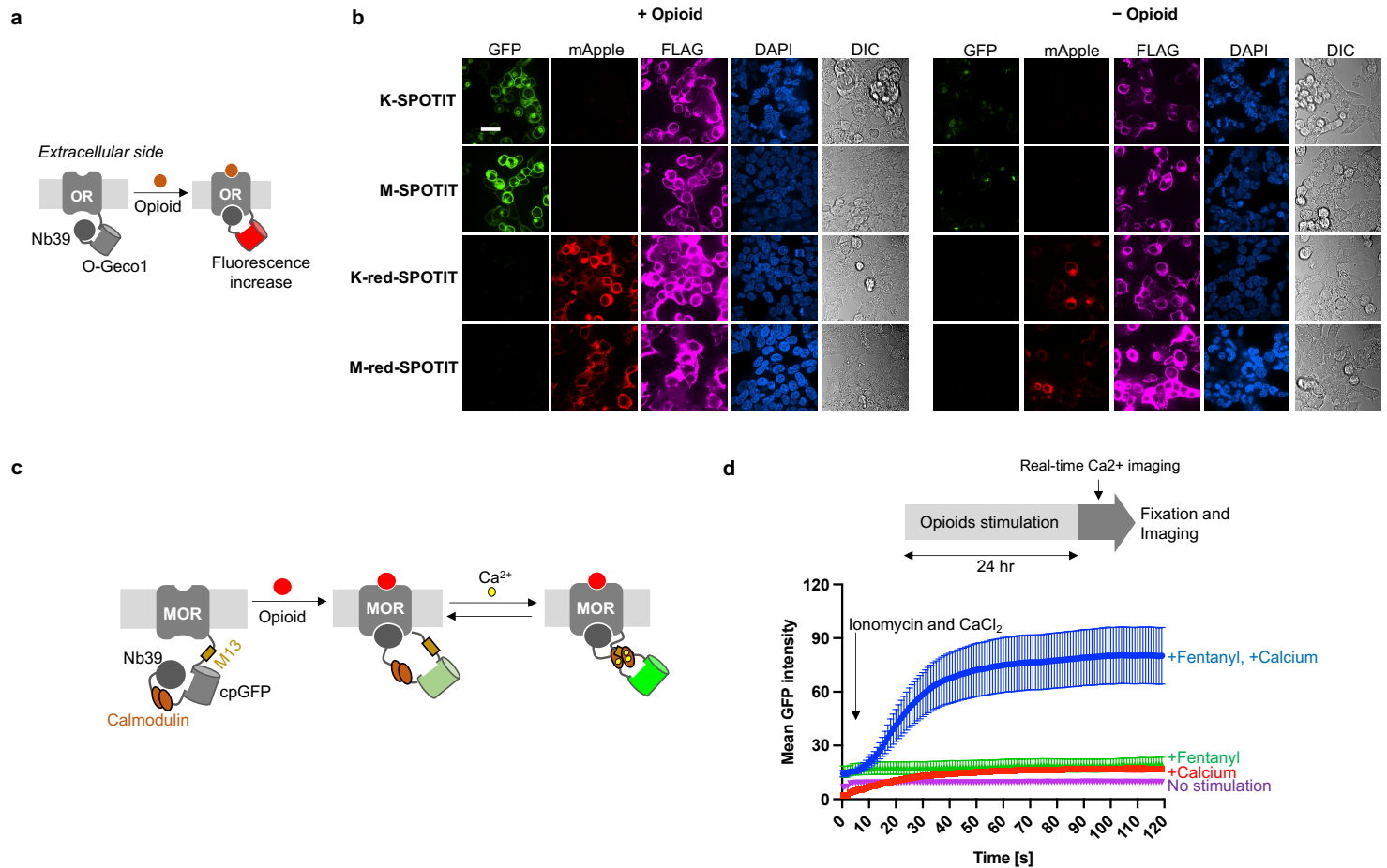


Fig. 3: red-SPOTIT and SPOTcal design and testing. **a**, Schematic of red-SPOTIT design. O-Geco1 replaces cpGFP from the original SPOTIT design. Nb39 inhibits O-Geco1 fluorophore maturation. Opioid binding recruits Nb39 to the OR, allowing the O-Geco1 fluorophore to mature. **b**, HEK293T cell testing of green or red SPOTIT. SPOTIT expressing cells were stimulated with 10 μ M of fentanyl or salvinorin A for MOR or KOR, respectively. 24 hours post opioid stimulation, cells were fixed, immunostained, and imaged at pH 11. GFP, cpGFP fluorescence. mApple, cpmApple fluorescence. FLAG, protein expression level. DAPI, nuclear staining. DIC, differential interference contrast. Scale bar, 20 μ m. **c**, Schematic of the opioid-activated calcium sensor. Opioid binding allows the fluorophore to mature, where calcium binding leads to an increase in fluorescence in live cells. **d**, Schematic of SPOTcal testing and plot of the real-time fluorescence increase from calcium stimulation. HEK293T cells expressing the opioid-activated calcium sensor were stimulated with 10 μ M fentanyl 24 hours post transfection. 24 hours after fentanyl stimulation, cells were then imaged in real-time before and after addition of 5 mM calcium chloride and 2 μ M ionomycin. Controls were also performed without opioid or without calcium and ionomycin. Mean values of replicates are indicated by the dot and error bars are the SEM. $n = 30$.

410

411 **References**

412

- 413 1. B. Gacasan, S., L. Baker, D. & L. Parrill, A. G protein-coupled receptors: the evolution of
414 structural insight. *AIMS Biophys* **4**, 491–527 (2017).
- 415 2. Wang, J., Gareri, C. & Rockman, H. A. G-Protein–Coupled Receptors in Heart Disease. *Circ*
416 *Res* **123**, 716–735 (2018).
- 417 3. Szafran, K. *et al.* Potential role of G protein-coupled receptor (GPCR) heterodimerization
418 in neuropsychiatric disorders: A focus on depression. *Pharmacological Reports* **65**, 1498–
419 1505 (2013).
- 420 4. Huang, Y., Todd, N. & Thathiah, A. The role of GPCRs in neurodegenerative diseases:
421 avenues for therapeutic intervention. *Curr Opin Pharmacol* **32**, 96–110 (2017).
- 422 5. Sriram, K. & Insel, P. A. G Protein-Coupled Receptors as Targets for Approved Drugs: How
423 Many Targets and How Many Drugs? *Mol Pharmacol* **93**, 251–258 (2018).
- 424 6. Taber, K. H. & Hurley, R. A. WINDOWS TO THE BRAIN Volume Transmission in the Brain:
425 Beyond the Synapse. *J Neuropsychiatry Clin Neurosci* **26**, 1 (2014).
- 426 7. Dong, A. *et al.* A fluorescent sensor for spatiotemporally resolved imaging of
427 endocannabinoid dynamics in vivo. *Nat Biotechnol* **40**, 787–798 (2022).
- 428 8. Sun, F. *et al.* Next-generation GRAB sensors for monitoring dopaminergic activity in vivo.
429 *Nat Methods* **17**, 1156–1166 (2020).
- 430 9. Wan, J. *et al.* A genetically encoded sensor for measuring serotonin dynamics. *Nat Neurosci*
431 **24**, 746–752 (2021).
- 432 10. Feng, J. *et al.* A Genetically Encoded Fluorescent Sensor for Rapid and Specific In Vivo
433 Detection of Norepinephrine. *Neuron* **102**, 745-761.e8 (2019).
- 434 11. Sun, F. *et al.* A Genetically Encoded Fluorescent Sensor Enables Rapid and Specific
435 Detection of Dopamine in Flies, Fish, and Mice. *Cell* **174**, 481-496.e19 (2018).
- 436 12. Jing, M. *et al.* A genetically encoded fluorescent acetylcholine indicator for in vitro and in
437 vivo studies. *Nat Biotechnol* **36**, 726–737 (2018).
- 438 13. Jing, M. *et al.* An optimized acetylcholine sensor for monitoring in vivo cholinergic activity.
439 *Nat Methods* **17**, 1139–1146 (2020).
- 440 14. Patriarchi, T. *et al.* An expanded palette of dopamine sensors for multiplex imaging in vivo.
441 *Nat Methods* **17**, 1147–1155 (2020).
- 442 15. Patriarchi, T. *et al.* Ultrafast neuronal imaging of dopamine dynamics with designed
443 genetically encoded sensors. *Science (1979)* **360**, (2018).
- 444 16. Zhang, Q., Zheng, Y. W., Coughlin, S. R. & Shu, X. A rapid fluorogenic GPCR– β -arrestin
445 interaction assay. *Protein Science* **27**, 874–879 (2018).
- 446 17. Kim, M. W. *et al.* Time-gated detection of protein-protein interactions with transcriptional
447 readout. *Elife* **e30233**, (2017).
- 448 18. Kroeze, W. K. *et al.* PRESTO-Tango as an open-source resource for interrogation of the
449 druggable human GPCRome. *Nat Struct Mol Biol* **22**, 362–369 (2015).
- 450 19. Lee, D. *et al.* Temporally precise labeling and control of neuromodulatory circuits in the
451 mammalian brain. *Nat Methods* **14**, 495–503 (2017).

- 452 20. Kroning, K. E. & Wang, W. Genetically encoded tools for in vivo G-protein-coupled receptor
453 agonist detection at cellular resolution. *Clin Transl Med* **12**, (2022).
- 454 21. Kroning, K. E. & Wang, W. Designing a Single Protein-Chain Reporter for Opioid Detection
455 at Cellular Resolution. *Angewandte Chemie - International Edition* **60**, 13358–13365
456 (2021).
- 457 22. Kroning, K. E., Li, M., Petrescu, D. I. & Wang, W. A genetically encoded sensor with
458 improved fluorescence intensity for opioid detection at cellular resolution. *Chemical*
459 *Communications* **57**, 10560–10563 (2021).
- 460 23. Chen, T. W. *et al.* Ultrasensitive fluorescent proteins for imaging neuronal activity. *Nature*
461 **499**, 295–300 (2013).
- 462 24. Huang, W. *et al.* Structural insights into μ -opioid receptor activation. *Nature* **524**, 315–321
463 (2015).
- 464 25. Emrick, M. A., Sadilek, M., Konoki, K. & Catterall, W. A. β -adrenergic-regulated
465 phosphorylation of the skeletal muscle Ca v1.1 channel in the fight-or-flight response. *Proc*
466 *Natl Acad Sci U S A* **107**, 18712–18717 (2010).
- 467 26. Rasmussen, S. G. F. *et al.* Structure of a nanobody-stabilized active state of the β 2
468 adrenoceptor. *Nature* **469**, 175–181 (2011).
- 469 27. Kruse, A. C. *et al.* Activation and allosteric modulation of a muscarinic acetylcholine
470 receptor. *Nature* **504**, 101–106 (2013).
- 471 28. Wu, J. *et al.* Improved orange and red Ca²⁺ indicators and photophysical considerations
472 for optogenetic applications. *ACS Chem Neurosci* **4**, 963–972 (2013).
- 473 29. Oh, J., Lee, C. & Kaang, B.-K. Imaging and analysis of genetically encoded calcium indicators
474 linking neural circuits and behaviors. *The Korean Journal of Physiology & Pharmacology* **23**,
475 237 (2019).
- 476 30. Montandon, G. *et al.* PreBötzing complex neurokinin-1 receptor-expressing neurons
477 mediate opioid-induced respiratory depression. *Journal of Neuroscience* **31**, 1292–1301
478 (2011).
- 479 31. Kroning, K. E. *et al.* A Modular Fluorescent Sensor Motif Used to Detect Opioids, Protein–
480 Protein Interactions, and Protease Activity. *ACS Chem Biol* **17**, 2212–2220 (2022).
- 481 32. Binkowski, B. F. *et al.* A luminescent biosensor with increased dynamic range for
482 intracellular cAMP. *ACS Chem Biol* **6**, 1193–1197 (2011).
- 483 33. Koehl, A. *et al.* Structure of the μ -opioid receptor-Gi protein complex. *Nature* **558**, 547–
484 552 (2018).
- 485 34. Das, A. T., Tenenbaum, L. & Berkhout, B. Tet-On Systems For Doxycycline-inducible Gene
486 Expression. *Curr Gene Ther* **16**, 156–167 (2016).
- 487 35. Angelopoulos, T. J. *et al.* *Endogenous opioids may modulate catecholamine secretion*
488 *during high intensity exercise. Eur J Appl Physiol* vol. 70 (1995).
- 489 36. Borg, P. J. & Taylor, D. A. Involvement of μ - and δ -opioid receptors in the effects of
490 systemic and locally perfused morphine on extracellular levels of dopamine, DOPAC and
491 HVA in the nucleus accumbens of the halothane-anaesthetized rat. *Naunyn-*
492 *Schmiedeberg's Arch Pharmacol* **355**, 582–588 (1997).

495 **Methods**

496

497 **Plasmids, cloning, and virus preparation.** Constructs were cloned in an ampicillin-resistant
498 adeno-associated viral vector with a CAG promoter. Standard cloning procedures, such as Q5 or
499 Taq polymerase PCR amplification, NEB restriction enzyme digest, and T4 ligation or Gibson
500 assembly were used. Heat shock transformation with XL1-blue competent cells was used for
501 transformation of plasmids. To prepare concentrated AAV1/2 virus, the protocol described in Shen
502 et al. was used.

503

504 Reference: Shen, J. *et al.* A general method for chemogenetic control of peptide function. *Nature*
505 *Methods* **20**, 112-122 (2023).

506

507 **HEK293T cell culture and transfection.** Complete growth media was used for HEK293T cell
508 culture. Complete growth media includes: 1:1 DMEM (Dublecco's Modified Eagle medium,
509 GIBCO): MEM (Modified Eagle medium, GIBCO), 10% FBS (Fetal Bovine Serum, Sigma), 1%
510 (v/v) penicillin-streptomycin (Gibco).

511 Cells were plated at a density so that they would reach 80-90% confluence on the day of
512 transfection. Cells were cultured at 37 °C under 5% CO₂.

513

514 For transfection, we pre-treated 48-well plastic plates with 200 µL of 20 µg/mL human fibronectin
515 (Milipore Sigma) for 10 minutes at 37 °C under 5% CO₂. After 10 minutes, we removed the
516 fibronectin and added 200 µL of 80-90% confluent HEK293T cells into each well. To prepare the
517 transfection mixture for each well, we combined 100 ng of DNA with 1 µL of PEI MAX solution
518 (polyethylenimine, Polysciences) in 10 µL of DMEM and incubated at room temperature for 10
519 minutes. After the incubation, we added 100 µL of complete growth media to the DNA-PEI MAX
520 mixture and mix it with the cell suspension in the well. Cells were incubated at 37 °C with 5% CO₂
521 until stimulation 20-24 hours later.

522

523 **HEK293T cell fixation and immunostaining.** Cells were removed and 100 µL of 4%
524 formaldehyde was added per well. Formaldehyde was incubated for 20 minutes at room
525 temperature and then removed. The wells were then washed twice with phosphate buffer saline
526 (PBS). After fixation, the cells were permeabilized using 100 µL of prechilled methanol per well
527 and incubated at -20 °C for 5 minutes. The wells were then washed twice with PBS. For
528 immunostaining, 1:1000 chicken anti-GFP antibody (primary antibody) and 1:1000 anti-chicken-
529 647 (secondary antibody) were diluted in PBS with 1% BSA. 100 µL of primary antibody was
530 added to each well and then the plate was rocked at room temperature for 30 minutes. After 30
531 minutes, the cells were washed twice with PBS and antibody staining was repeated with the
532 secondary antibody. After 30 minutes of secondary antibody rocking, the cells were washed twice
533 with PBS and then fixed with 4% formaldehyde again for 20 minutes at room temperature. After
534 20 minutes, the cells were washed 2x with PBS and then 200 µL of pH 11 CAPS buffer was added
535 to the cells, except for the cells for the pH titration. For experiments with red fluorescent proteins,
536 mouse anti-FLAG and anti-mouse-647 primary and secondary antibodies, respectively, were
537 used following the same dilutions and procedure.

538

539 **Confocal microscopy of HEK293T cells.** Confocal imaging was performed on a Nikon inverted
540 confocal microscope with 20x air objective and 60x oil immersion objective, outfitted with a
541 Yokogawa CSU-X1 5000RPM spinning disk confocal head, and Ti2-ND-P perfect focus system
542 4, a compact 4-line laser source: 405 nm (100 mW) 488 nm (100 mW), 561 nm (100mW) and
543 640-nm (75 mW) lasers. The following combinations of laser excitation and emission filters were
544 used for various fluorophores: EGFP/Alexa Fluor 488 (488 nm excitation; 525/36 emission),

545 mCherry (568 nm excitation; 605/52 emission), Alexa Fluor 647 (647 nm excitation; 705/72
546 emission), and differential interference contrast (DIC). The acquisition time for all images was 1
547 second with 50% laser power intensities. ORCA-Flash 4.0 LT+sCMOS camera. 20x objective or
548 60x objective was used for all HEK293T cell experiments. 10x objective was used for mouse brain
549 slice images. All images were collected using Nikon NIS-Elements hardware control and
550 processed using NIS-Elements General Analysis 3 software.

551
552 **Analysis of HEK293T cell and animal images.** For all HEK293T cell experiments, three
553 technical replicates were performed (three wells for each condition.) 10 images were taken per
554 well, and the sum intensity value was measured for each image. The sum intensity value was
555 taken using the NIS-Elements General Analysis 3 software. Specifically, a threshold value was
556 set to be above the autofluorescence of the cells, where only real cpGFP/cpRFP fluorescence
557 signal would be measured. The threshold was generally set to be 1.5-2x higher than the
558 autofluorescence from the plate void of cells. The same threshold was used for all conditions in a
559 single experiment. Two values were taken from the cells that have fluorescence values within the
560 threshold: the mean intensity value and the total object area of the field of view. The total object
561 area is the area of cells that fit in the threshold and the mean intensity value is the mean intensity
562 value of the cells counted in the total object area. The total object area was then multiplied by the
563 mean intensity value to calculate the sum intensity value.

564
565 For background subtraction of HEK293T cell experiments, the mean intensity value of the plate
566 by itself (area with no cells) was multiplied by the object area and then subtracted from the sum.
567 For background subtraction of mouse experiments, the mean intensity value of the region of the
568 brain away from the injection site was multiplied by the object area and then subtracted from the
569 sum. For all HEK293T cell experiments and the M-SPOTIT2 mouse experiment, one background
570 value for subtraction was used for each experiment. For mouse testing of B2AR-SPOTall, we
571 performed different background subtractions depending on the background of each individual
572 image. This was because the dimmer fluorescent signal of B2AR-SPOTall is more impacted by
573 tissue autofluorescence.

574
575 For HEK293T cell experiments, the sum intensity values for the 10 images from each technical
576 replicate were averaged and then each technical replicate was plotted as one point in the graph.
577 For the mouse experiments, sum intensity values were calculated for each individual image. The
578 mean of the sum intensity for the 5 brightest images from each mouse was calculated and plotted
579 as one point in the graph. For all experiments, Prism GraphPad software was used for plotting,
580 as well as performing unpaired two-sided Student's t tests to calculate significance. All images
581 were included in analysis, except for images that had lower than a 50% cell density in the image,
582 were blurry, or had auto fluorescent artifacts. Images excluded from analysis are indicated in the
583 data sheets included in the submission.

584
585 **B2AR-SPOTall initial testing and engineering.** 20-24 hours after transfection, HEK293T cells
586 were stimulated with 100 μ L of isoproterenol diluted in complete growth media, where there would
587 be a 10 μ M final concentration within the well. 24 hours after stimulation, the cells were fixed,
588 immunostained, and imaged with a CAPS pH 11 buffer following the above protocols. 60x imaging
589 was performed using glass bottom plates (Corning).

590
591 **B2AR-SPOTall agonist exposure experiment.** 20-24 hours after transfection, HEK293T cells
592 were stimulated with 100 μ L of isoproterenol diluted in complete growth media to a 10 μ M final
593 concentration within the well. Cells were incubated with isoproterenol for either 30 seconds, 5
594 minutes, 6 hours, and 24 hours. After the indicated exposure time, the cells were washed 2x with

595 complete growth media and then incubated without agonist for 24 hours. The cells were then fixed
596 and imaged at 20x with a CAPS pH 11 buffer following the above protocol.

597

598 **B2AR-SPOTall maturation experiment.** HEK293T cells were transfected with B2AR-SPOTall
599 DNA for all conditions at the same time. The 24-hour time point was stimulated 24 hours before
600 imaging (24 hours after transfection) with 100 μ L of isoproterenol diluted in complete growth
601 media to a 50 μ M final concentration within the well. After 5 minutes of isoproterenol incubation,
602 the cells were washed 2x with complete growth media. The 8, 6, 4, 3, 2, 1.5, 1, and 0.5-hour time
603 points were stimulated 8, 6, 4, 3, 2, and 1.5 hours before imaging. After stimulation and washing,
604 the cells were incubated without drug at 37 °C under 5% CO₂. All cells were fixed and imaged at
605 the same time to minimize protein level differences between conditions. Cells were imaged at 20x
606 magnification with a CAPS pH 11 buffer.

607

608 **B2AR-SPOTall pH titration.** 24 hours after transfection with B2AR-SPOTall DNA, HEK293T cells
609 were stimulated with 10 μ M isoproterenol for 5 minutes. The cells were then washed 2x with
610 complete growth media and incubated for 24 hours in complete growth media without drug at 37
611 °C under 5% CO₂. The cells were then fixed and imaged with buffers of different pH. pHs: 5.61,
612 6.96, 7.66, 8.06, 8.62, 9.12, 10.25, and 11.01. 100 mM Tris-HCl, 100 mM CAPS, and 1x PBS
613 buffers were used. Cells were imaged at 20x magnification.

614

615 **B2AR-SPOTall selectivity.** 24 hours after transfection with B2AR-SPOTall DNA, HEK293T cells
616 were stimulated with different agonists to give a 50 μ M final concentration. The agonists were
617 diluted in complete growth media and added for 5 minutes. After 5 minutes of agonist incubation,
618 the wells were washed 2x with complete growth media, and the cells were incubated without drug
619 at 37 °C under 5% CO₂. 24 hours after stimulation, the cells were fixed and imaged at 20x
620 magnification with a CAPS pH 11 buffer.

621

622 **CHRM2- and DRD1-SPOTall initial testing.** HEK293T cells expressing the CHRM2- or DRD1-
623 SPOTall sensors were stimulated with iperexo and dopamine, respectively to a final concentration
624 of 100 μ M. After stimulation, the cells were incubated at 37 °C under 5% CO₂ for 24 hours. Then,
625 the cells were fixed, immunostained, and imaged at both 60x and 20x magnifications with a CAPS
626 pH 11 buffer. Glass bottom plates were used.

627

628 **M- and K- red-SPOTIT initial testing and engineering.** HEK293T cells expressing the M- and
629 K-red SPOTIT sensors were stimulated with fentanyl or salvinorin A, respectively, to a final
630 concentration of 10 μ M. After stimulation, the cells were incubated at 37 °C under 5% CO₂ for 24
631 hours. Then, the cells were fixed, immunostained, and imaged at both 60x and 20x magnifications
632 with a CAPS pH 11 buffer. Glass bottom plates were used.

633

634 **B2AR-SPOTall agonist titrations.** HEK293T cells expressing B2AR-SPOTall were stimulated
635 with varying concentrations of the following drugs: epinephrine, isoproterenol, arformoterol,
636 indacaterol, levalbuterol, and butoxamine. Serial dilutions were performed, where the drug was
637 diluted in complete growth media. Drug was added to the well for 5 minutes and then the wells
638 were washed 2x with complete growth media. After stimulation, the cells were incubated at 37 °C
639 under 5% CO₂ for 24 hours without drug. Then, the cells were fixed and imaged at 20x
640 magnification with a CAPS pH 11 buffer.

641

642 **Calcium-Gated SPOTIT.** HEK293T cells expressing SPOTcal were stimulated with fentanyl
643 diluted in complete growth media to a final concentration of 10 μ M. After stimulation, the cells
644 were incubated at 37 °C under 5% CO₂ for 18 hours. For calcium and ionomycin stimulation, 100

645 μL of ionomycin and CaCl_2 diluted in pre-warmed complete growth media were added to the wells
646 to a final concentration of 2 μM and 5 mM, respectively. Images were taken every 1 second for 2
647 minutes immediately before and after calcium stimulation. 20x magnification imaging was used.

648

649 **Gai binding site mutations testing**

650

651 *cAMP Assay.* 100 ng of SPOTIT DNA and 50ng of GloSensor DNA (Promega) was used for
652 transfection. 20 hours after transfection, the complete growth media in the well was replaced with
653 100 μL of 2 mM D-luciferin potassium salt (Gold Bio, #LUCK) in complete growth medium (with
654 50 mM HEPES). Luminescence values were measured using a plate reader (BioTek, CYTATION
655 5). Luminescence values were measured for 1 hour, after which cells were treated with 1 μL of
656 100 μM forskolin (Sigma-Aldrich, #F6886) in complete growth media. Luminescence values were
657 measured for 30 min, and then the opioid condition cells were treated with 1 μL of 1 mM fentanyl
658 (for mu-opioid receptor constructs) or 1 μL of 1 mM Sal A (for kappa-opioid receptor constructs)
659 in complete growth media. Luminescence values were measured for 30 min.

660

661 *Confocal Microscopy.* 24 hours after transfection of the SPOTIT sensors, HEK293T cells were
662 stimulated with 100 μL of salvinorin A (for kappa-opioid receptor constructs) or fentanyl (for mu-
663 opioid receptor constructs) diluted in complete growth media to a final concentration of 10 μM .
664 After stimulation, the cells were incubated at 37 °C for 20 hours and then fixed and imaged at 20x
665 with a CAPS pH 11 buffer.

666

667 **Mouse Lines.** All procedures were carried out in accordance with the animal care standards in
668 National Institutes of Health (NIH) guidelines and approved by the University Committee on Use
669 and Care of Animals at the University of Michigan. Animals were maintained on a 12 hours
670 light/dark cycle with ad libitum access to food and water. All mice strains utilized were C57BL/6J
671 genetic background.

672

673 **M-SPOTIT2 mouse testing**

674

675 *Stereotactic injection.* Adult mice were anesthetized with isoflurane (4 - 5% for induction, 1.5% for
676 maintenance) for stereotactic injection. Animals received 5 mg/kg of preemptive analgesic
677 carprofen prior to placement in the stereotactic frame (David Kopf Instruments) and body
678 temperature was maintained at 35 – 37 °C using a feedback-controlled heating pad (Physitemp,
679 TCAT-2LV). The following coordinates were used for injection: PreBotC, \pm 1.3 mm from the
680 midline; - 6.7 mm posterior to the bregma, -6.1 mm ventral from bregma. 500nL of the AAV1/2-
681 CAG-M-SPOTIT2 virus was injected into the PreBotC at a rate of 50nL/min.

682

683 *Opioid administration and histology.* 6 days after injection of the viral vectors into the mouse brain,
684 100mg/kg of morphine or saline was administered through intraperitoneal injection. Twenty-four
685 hours after drug or saline administration, the mice were deeply anesthetized and transcardially
686 perfused with 10 mL PBS, followed by 10 mL 4% paraformaldehyde (PFA). The brain tissue was
687 removed and post-fixed overnight at 4 °C in 4 % PFA and then cryopreserved in 30% sucrose for
688 48 hours. The processed tissue was then embedded into optimum cutting temperature compound
689 (OCT) and sectioned into serial slices through the relevant region at 40 microns with a Leica
690 cryostat CM3050 S cryostat.

691

692 For immunostaining, sections were washed in 0.1% PBS Tween 20 (PBS with 0.1% Tween 20)
693 and permeabilized with 0.3% PBS Triton X-100 for 30 min, followed by 2% bovine serum albumin
694 (BSA) blocking solution at room temperature for 1 hour. Sections were then incubated with
695 primary antibody (Chk pAb to GFP; Abcam13970; 1:500 dilution; Lot: GR3361051-18) in BSA

696 overnight at 4 °C. After washing in 0.1% PBS Tween 20 three times (5 minutes each time),
697 sections were incubated with secondary antibody (Alexa Fluor 647 goat anti- chicken IgG; Life
698 technologies A21449; 1:500 dilution; Lot: 1599393) for 2 hrs. After washing in 0.1% PBS Tween
699 20 three times (5 min each time), sections were then stained with 4',6 -diamidino-2-phenylindole,
700 dihydrochloride (DAPI; Invitrogen; D1306) diluted 1:10000 in PBS. After washing in 0.1% PBS
701 Tween 20 three times (5 minutes each time), sections were imaged on a confocal microscope
702 with pH 11 buffer.

703

704 **B2AR-SPOTall mouse testing**

705

706 *Stereotactic injection of AAV into the mouse brain.* The procedure of stereotactic injection was
707 described in previous work. Adult mice were anesthetized with isoflurane (5% for induction, 1.5%
708 for maintenance), administered 5 mg kg⁻¹ of carprofen, prior to being placed in a stereotactic
709 apparatus. The mice's shaved heads were disinfected using one application of betadine and three
710 applications of alcohol pad. The body temperature of the was monitored and maintained at 35 °C.
711 A total of 400 nl of concentrated AAV1/2-CAG-B2AR-SPOTall were injected into the lateral
712 hypothalamic area (0.95 mm lateral to midline, -1.40 mm posterior, and -5.25 mm ventral to
713 bregma) at a rate of 50nl min⁻¹ for 8 minutes. After injection, the pipette was left in the brain for
714 10 minutes to allow for pressure to equalize.

715

716 *Isoproterenol, epinephrine administration and histology.* After the injection of the viral vectors into
717 mouse brain, a local injection of 1 µl 10 mM Isoproterenol, epinephrine, or saline (Hospira,
718 #00409-4888-10) control was administered into LHA via stereotactic injection seven days later.
719 Twenty-four hours after local injection of drugs or saline, the animals were euthanized and
720 perfused with PBS and 4% paraformaldehyde (PFA, Electron Microscopy Science, #15713). The
721 brain tissues were collected and post-fixed overnight in 4% PFA then cryoprotected in 30%
722 sucrose for 48 hours at 4 °C. The fixed tissue was then embedded in optimum cutting temperature
723 compound, sectioned at 40 µm, and mounted onto glass slides. To prepare the tissue sections
724 for immunostaining, tissue sections were first incubated in 0.3% Triton (Sigma, #T8787) in PBS
725 for 30 minutes, followed by blocked in 2% BSA (Sigma, #A9647) in 0.1% Tween-20 in PBS for
726 1 hour. Next, the sections were incubated with chicken anti-GFP antibody (1:500, abcam,
727 #ab13970) in 2% BSA overnight at 4 °C. After three washes with 0.1% Tween-20 for 5 minutes
728 each, the sections were incubated with donkey anti-chicken Alexa Fluor 647 antibody (1:500,
729 Invitrogen, #A78952) for 2 hours at room temperature. The tissue sections were then rinsed in
730 0.1% PBS Tween-20 and stained with DAPI (1:10,000, Invitrogen, #D1306) for 10 minutes at
731 room temperature, and fixed with pH 11 PBS for 20 minutes. Finally, Confocal images were
732 captured using a Nikon A1 Confocal microscope with pH 11 buffer.

733

734 **Respiratory Recording.** Morphine was prepared in sterile saline at a concentration at 10 mg/mL
735 and delivered at a dose of 100 mg/kg. To test the respiratory depression of morphine, individual
736 mice were placed in a 450 mL whole-body plethysmography (WBP) chamber at room temperature
737 (22°C). Mice were allowed to acclimate to the chamber for 30 minutes before the respiratory
738 parameters were recorded by Emka IOX2 software (EMKA Technologies, Paris, France). Animals
739 then underwent a 15 minutes baseline recording before a 200 µL IP injection of sterile saline.
740 Following the injection, mice underwent an additional 30 minutes recording and then returned to
741 their home cage for 20 minutes. Mice were then returned to the WBP for a 15-minutes baseline
742 recording before an IP injection of morphine. Following the injection, the mice were recorded for
743 an additional 30 minutes.